New Azastannatranes: Substitution at the Axial Amide Bond

Winfried Plass[†] and John G. Verkade[*]

Department of Chemistry, Iowa State University, Ames, Iowa 50011

Received April 15, 1993[●]

The reactivity of the azastannatrane $Me_2NSn(NMeCH_2CH_2)_3N$ (**1**) against protolytic reagents was investigated. The axial NMe_2 group of **1** is labile to substitution, affording a variety of new azastannatrane derivatives $ZSn-(NMeCH_2CH_2)_3N$ where Z is F (**9**), Cl (**10**), Br (**11**), I (**12**), $^1/_2(C{\equiv}C)$ (**13**), and $PhC{\equiv}C-$ (**14**). Variable temperature ^1H NMR spectroscopy was used to study the mobility of the azastannatrane framework. The FT-IR spectra of the series of new azastannatranes **8–11** also provide insight into the vibrational motion of such frameworks. ^{119}Sn NMR spectroscopy in solution as well as in the solid state indicates the presence of a strong transannular tin–nitrogen bond. In the CP/MAS ^{119}Sn NMR spectrum of **9**, effects due to coupling with the quadrupolar chlorine nucleus are observed. Crystal data for **1**: orthorhombic space group, *Pnma*, $a = 15.855(3)$ Å, $b = 11.895(2)$ Å, $c = 8.410(2)$ Å, and $Z = 4$.

Introduction

Recently we described the synthesis of a series of new azastannatranes **1–7** via transamination reactions of $RSn(NMe_2)_3$
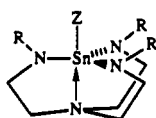
1 Z = NMe₂, R = Me	**9** Z = F, R = Me
2 Z = Me, R = H	**10** Z = Cl, R = Me
3 Z = Me, R = Me	**11** Z = Br, R = Me
4 Z = *n*-Bu, R = H	**12** Z = I, R = Me
5 Z = *n*-Bu, R = Me	**13** Z = 1/2(C≡C), R = Me
6 Z = Ph, R = H	**14** Z = C≡CPh, R = Me
7 Z = Ph, R = Me	
8 Z = 1/2O, R = Me	

with tris(2-aminoethyl)amine (tren) and its methyl-substituted derivative (Me-tren).[1] These azastannatranes were found to undergo a facile transmetalation reaction with transition metal alkoxides, thereby transferring the atrane framework onto the transition metal.[2] We therefore became interested in additional insight into the reactivity of azastannatranes.

The reaction of aminostannanes with protic species was studied early on by Lappert et al. in 1965.[3] These compounds were found to react according to eq 1 with a wide range of protic reagents.

$$R_3SnNR'_2 + HA \rightarrow R_3SnA + R'_2NH \qquad (1)$$

Lappert and co-workers also reported on methatetical reactions of aminostannanes with a wide variety of substrates.[4] In a preliminary study of reaction 1 with azastannatrane **1**, we probed its reactivity with the protic species H_2O.[1] Interestingly, **1** was found to react with traces of water to displace its apical dimethylamino group forming the oxygen-bridged bis(azastannatrane) **8**.

In this paper we report on the displacement of the apical Me_2N group in **1** by a series of protic reagents to give azastannatranes **9–14** and on the structural and spectroscopic properties of these new compounds.

Experimental Section

All manipulations were carried out in an atmosphere of dry argon under strict exclusion of moisture, using standard vacuum line techniques. Solvents were purified by standard methods[5] and distilled prior to use.

† New address: Facultät für Chemie, Universität Bielefeld, Postfach 100131, 4800 Bielefeld 1, Germany.
● Abstract published in *Advance ACS Abstracts*, October 1, 1993.
(1) Plass, W.; Verkade, J. G. *Inorg. Chem.*, preceding paper in this issue.
(2) Plass, W.; Verkade, J. G. *J. Am. Chem. Soc.* **1992**, *114*, 2275.
(3) Jones, K.; Lappert, M. F. *J. Organomet. Chem.* **1965**, *3*, 295.
(4) George, T. A.; Lappert M. F. *J. Chem. Soc. A* **1969**, 992.
(5) Perrin, D. D.; Armarego, W. L. F. *Purification of Laboratory Chemicals*, 3rd ed.; Pergamon Press: Oxford, New York, Frankfurt, 1988.

Samples for IR and solid-state NMR experiments were prepared in a drybox with a dry oxygen-free nitrogen atmosphere. 1-(Dimethylamino)-*N,N',N''*-trimethylazastannatrane (**1**) was prepared as described earlier.[1] Microanalyses were carried out by Galbraith Laboratories, Knoxville, TN, and Desert Analytics, Tucson, AZ.

High-resolution mass spectral data were recorded on a Kratos MS50 mass spectrometer with electron impact ionization (70 eV) by peak matching. Low-resolution MS measurements were carried out on a Finnigan 4000 instrument using CI (NH_3) as well as FAB techniques. IR spectra were recorded on an IBM98 FT-IR spectrometer as KBr pellets (4000–600 cm⁻¹) and as Nujol mulls between polyethylene plates (650–150 cm⁻¹).

Solution NMR spectra were recorded on a Varian VXR300 (^1H, 299.95 MHz; ^{13}C, 75.43 MHz; ^{119}Sn, 111.92 MHz) and a Bruker WM200 (^{119}Sn, 74.63 MHz) instrument using deuterated solvents as internal locks and TMS (^1H, ^{13}C) and $SnMe_4$ (^{119}Sn) as external standards. For solid state NMR spectra, glycine (^{13}C) and tetracyclohexylstannane (^{119}Sn)[6] were used as secondary references. As a solvent for low-temperature experiments, toluene-d_8 was used. Temperature calibration of the NMR probe was carried out by literature methods.[7] For the acquisition of solid-state NMR spectra, polycrystalline samples (ca. 300–400 mg) were packed either into an airtight insert or directly into a ZrO_2 rotor which was sealed by a threaded Teflon plunger. Spectra were obtained on a Bruker MSL300 spectrometer (^{13}C, 75.47 MHz; ^{119}Sn, 111.92 MHz) under proton decoupling using the CP/MAS technique, with spectral widths of 10–25 (^{13}C) and 100 kHz (^{119}Sn). A 90° pulse was employed, and cross polarization contact times of 2–3 ms were used, followed by a recycle delay of 6 s. Spinning rates were in the range 2.0–4.5 kHz. Spectra were generally rerun at different sample spinning rates to establish the position of the centerband.

1-Z-*N,N',N''*-trimethylazastannatranes with Z = F, Cl, Br, and I (9–12). To a stirred solution of **1** in THF (ca. 25 mL/mmol) was added 1 equiv of an ammonium salt. In the case of **9**, NEt_3·3HF was added dropwise whereas, for **10–12**, the neat NEt_3HX was added in one portion. After 2 h of stirring at room temperature, the precipitate that formed was removed by filtration and extracted with the same solvent. After the solvent was stripped off in vacuo, the resulting colorless microcrystalline solid was washed with *n*-pentane and dried in vacuo.

9. Yield: 0.37 g (95%). Mp: dec > 160 °C; MS (70 eV, EI): *m/e* 320.076 45, < 1% (calcd for $C_9H_{21}FN_4^{116}Sn$ (M⁺), 320.07 713). IR (cm⁻¹): 190 (w), 271 (w), 284 (vw), 302 (w), 406 (w), 510 (w), 515 (m), 571 (w), 581 (w), 620 (vw), 731 (sh), 746 (m), 822 (m), 841 (m), 872 (m), 882 (sh), 922 (m), 1016 (vs), 1036 (vs), 1046 (sh), 1065 (m), 1113 (s), 1121 (sh), 1156 (vs), 1160 (sh), 1202 (s), 1219 (sh), 1242 (m), 1273 (m), 1283 (m), 1340 (m), 1350 (s), 1387 (m), 1423 (m), 1443 (s), 1468 (s), 1481 (m), 1504 (w), 2664 (m), 2781 (vs), 2839 (vs), 2860 (vs), 2905 (s), 2941 (s), 2953 (s), 2970 (s). ^{19}F NMR (C_6D_6): 70.57 ppm, $^1J_{SnF}$ = 2917, 2788 Hz (^{119}Sn, ^{117}Sn).

(6) Harris, R. K.; Sebald, A. *Magn. Reson. Chem.* **1987**, *25*, 1058.
(7) Martin, M. L.; Delpuech, J. J.; Martin, G. J. *Practical NMR Spectroscopy*; Heyden: London, 1980.

10. Yield: 1.13 g (90%). Mp: dec 127–128 °C. Anal. Calcd (found) for $C_9H_{21}ClN_4Sn$: C, 31.85 (32.30); H, 6.24 (6.52); Cl, 10.44 (10.54); N, 16.51 (16.42); MS (70 eV, EI): m/e 336.046 82, 1% (calcd for $C_9H_{21}ClN_4{}^{116}Sn$ (M⁺) 336.047 57). IR (cm⁻¹): 282 (sh), 304 (m), 404 (w), 484 (w), 512 (w), 568 (w), 580 (w), 620 (vw), 736 (sh), 746 (m), 839 (s), 870 (m), 877 (sh), 922 (m), 1013 (vs), 1034 (vs), 1061 (m), 1086 (m), 1109 (s), 1126 (sh), 1140 (vs), 1154 (sh), 1198 (s), 1217 (m), 1240 (m), 1275 (m), 1310 (w), 1340 (sh), 1350 (s), 1369 (m), 1420 (m), 1445 (s), 1464 (s), 1473 (sh), 2664 (m), 2678 (m), 2781 (vs), 2843 (vs), 2868 (vs), 2932 (s), 2963 (s).

11. Yield: 1.58 g (94%). Mp dec 128–129 °C; MS (70 eV, EI): m/e 379.996 30, < 1% (calcd for $C_9H_{21}{}^{79}BrN_4{}^{116}Sn$ (M⁺) 379.997 06). IR (cm⁻¹): 200 (sh), 225 (vw, br), 284 (vw, br), 305 (vw), 397 (w), 480 (w), 508 (w), 568 (w), 588 (vw), 618 (vw), 726 (m), 748 (m), 831 (sh), 841 (m), 870 (m), 882 (w), 902 (vw), 924 (m), 1003 (sh), 1018 (vs), 1042 (vs), 1067 (s), 1082 (s), 1111 (s), 1126 (s), 1138 (s), 1148 (sh), 1196 (s), 1234 (w), 1277 (m), 1282 (sh), 1304 (m), 1342 (sh), 1352 (m), 1375 (w), 1424 (sh), 1448 (s), 1455 (sh), 1470 (s), 2665 (m), 2781 (vs), 2844 (vs), 2867 (sh), 2930 (s), 2964 (s).

12. Yield: 1.22 g (87%). Mp: dec 124–125 °C. MS (CI, NH₃): m/e ([M + 4NH₃]⁺); with EI no M⁺ peak was observed. IR (cm⁻¹): 189 (vw), 206 (w), 228 (sh), 281 (w, br), 306 (w, br), 394 (w, br), 441 (w), 475 (w), 502 (w), 568 (w), 597 (w), 621 (vw), 726 (m), 750 (m), 822 (m), 839 (sh), 872 (m), 880 (sh), 926 (m), 1016 (vs), 1042 (vs), 1067 (m), 1100 (sh), 1111 (s), 1134 (vs), 1146 (sh), 1196 (s), 1220 (sh), 1242 (w), 1279 (m), 1344 (sh), 1354 (s), 1375 (w), 1418 (m), 1445 (s), 1460 (sh), 2667 (m), 2777 (vs), 2835 (vs), 2854 (vs), 2907 (s), 2961 (s).

Bis(N,N',N'-trimethylazastannatranyl)acetylene (13). A slow stream acetylene was bubbled through a solution of 3.52 g of **1** (10.1 mmol) in 50 mL of toluene. To remove water and acetone, the acetylene was passed through a Dry Ice cold trap and a drying tower filled with alumina. ¹¹⁹Sn NMR spectroscopy showed that, after 12 h of reaction time, all the starting material **1** was converted. After filtration, the solvent was removed in vacuo and the solid residue was extracted with *n*-pentane and recrystallized from toluene yielding 2.28 g (71%) of **13**. Mp: 194–195 °C; IR (cm⁻¹): 298 (w), 392 (vw), 431 (vw), 480 (w), 506 (m), 561 (m), 577 (m), 603 (sh), 656 (w), 733 (sh), 748 (m), 777 (w), 847 (s), 857 (sh), 881 (s), 926 (m), 1026 (vs), 1047 (vs), 1064 (sh), 1086 (m), 1113 (s), 1135 (sh), 1144 (vs), 1155 (sh), 1209 (s), 1244 (m), 1283 (s), 1302 (sh), 1342 (m), 1354 (s), 1377 (m), 1402 (m), 1420 (m), 1447 (s), 1462 (s), 1597 (w), 1641 (m), 1722 (w), 2669 (m), 2775 (vs), 2827 (vs), 2856 (vs), 2902 (s), 2924 (s), 2955 (s).

1-(Phenylacetylenyl)-N,N,N'-trimethylazastannatrane (14). A neat sample of 0.43 g of phenylacetylene (4.2 mmol) was added dropwise to a stirred solution of **1** (1.45 g, 4.2 mmol) in 50 mL of toluene. After the solution was stirred for ¹/₂ h at room temperature, the volatiles were removed in vacuo. Recrystallization of the crude product from toluene at –20 °C gave 0.90 g (52%) of colorless crystals. Mp: 74–75 °C. Anal. Calcd (found) for $C_{17}H_{26}N_4Sn$: C, 50.40 (49.65); H, 6.47 (6.25); N, 13.83 (13.50); MS (70 eV, EI): m/e 406.118 16, 2% (calcd for $C_{17}H_{26}N_4{}^{120}Sn$ (M⁺) 406.117 95); IR (cm⁻¹): 298 (w, br), 368 (vw), 391 (vw), 432 (vw), 482 (w), 507 (w), 519 (vw), 532 (w), 552 (w), 595 (w), 602 (vw), 623 (vw), 692 (s), 748 (m), 761 (s), 791 (m), 808 (w), 845 (m), 883 (s), 920 (m), 968 (w), 998 (sh), 1022 (vs), 1045 (vs), 1069 (m), 1111 (s), 1122 (sh), 1144 (vs), 1205 (s), 1240 (w), 1279 (sh), 1284 (s), 1340 (m), 1354 (s), 1377 (w), 1420 (m), 1445 (s), 1466 (m), 1485 (s), 1570 (w), 1597 (m), 2131 (m), 2669 (m), 2777 (vs), 2820 (vs), 2834 (vs), 2856 (vs), 2905 (s), 2949 (s), 2991 (w), 3047 (m), 3078 (w).

Crystal and Molecular Structure of 1-(Dimethylamino)-N,N,N'-trimethylazastannatrane (1). A glass capillary containing a colorless crystal of **1** under a nitrogen atmosphere was mounted on an Enraf-Nonius CAD4 diffractometer, and data were taken with graphite monochromated Mo Kα radiation. Pertinent data collection and reduction information are given in Table I, and positional parameters and their standard deviations are collected in Table II. Lorentz and polarization corrections were applied to the data, a nonlinear correction based on the decay of standard reflections was made, and an absorption correction based on a series of Ψ scans was applied. The structure was solved by direct methods.[8] Refinement calculations were performed on a Digital Equipment Corp. Vax Station 3100 computer using the SHELXTL-Plus programs.[8]

---

(8) SHELXTL-Plus, Siemens Analytical X-ray, Inc., Madison, WI.

Table I. Crystallographic Data for **1**

formula	$C_{11}H_{27}N_5Sn$
fw	348.1
space group	*Pnma*
a, Å	15.855(3)
b, Å	11.444(2)
c, Å	8.410(2)
V, Å³	1525.9(5)
Z	4
d_{calc}, g/cm³	1.515
cryst size, mm	$0.45 \times 0.40 \times 0.40$
μ(Mo Kα), mm⁻¹	1.665
radiation λ, pm (monochromated in incident beam)	7.1073
orientation reflcns: no.; range (2θ), deg	25, 21.2–28.5
temp, K	223
scan method	$2\theta–\theta$
data collecn range (2θ), deg	4.0–60.0
no. of data collcd	11 662
no. of unique data: tot. with $F_o{}^2 > 4\sigma(F_o{}^2)$	2451
no. of params refined	101
max, min transm factors (ψ scans)	0.7013, 0.8328
R^a	0.0328
$R_w{}^b$	0.0389
quality-of-fit indicator^c	1.95
largest shift/esd, final cycle	0.001
largest peak, 10³⁰ e/m^3	1.12

^{a} $R = \sum\|F_o| - |F_c\|/\sum|F_o|$. ^{b} $R_w = [w(|F_o| - |F_c|)^2/\sum w|F_o|^2]^{1/2}$; $w = 1/\sigma^2(|F_o|)$. ^{c} Quality-of-fit $= [\sum w(|F_o| - |F_c|)^2/(N_{observns} - N_{params})]^{1/2}$.
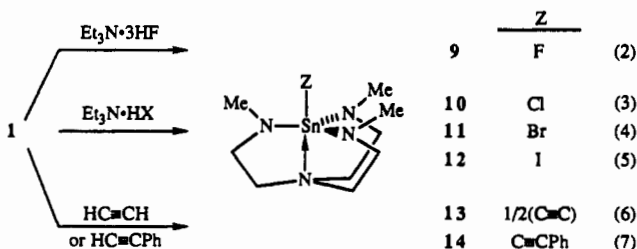
Table II. Positional Parameters and Their Standard Deviations for **1**

	x	y	z	$U(eq)^a$
Sn	1839(1)	2500	1674(1)	34(1)
N(4)	858(2)	2500	125(4)	48(1)
N(1)	2983(2)	2500	3488(3)	53(1)
C(2)	3684(3)	2500	956(3)	80(2)
C(7)	627(2)	1454(4)	−747(4)	69(1)
C(4)	2878(3)	1437(3)	4384(4)	68(1)
C(6)	787(2)	728(4)	3417(5)	73(1)
C(5)	2086(4)	1118(6)	4564(7)	52(2)
C(1)	3750(3)	2107(5)	2541(6)	45(1)
N(3)	1607(2)	986(3)	2878(4)	76(1)
C(3)	2841(4)	2500	−1434(5)	101(4)
N(2)	2878(2)	2500	252(3)	45(1)
C(5')	2349(4)	386(5)	3519(7)	51(2)

^{a} In units of Å² × 10³. Anisotropically refined atoms are given in the form of the equivalent isotropic U defined as one-third of the trace of the orthogonalized U_{ij} tensor.

Results and Discussion

Syntheses. The reaction of **1** with protic reagents according to eqs 2–7 gave the new azastannatranes **9–14**. These reactions

		Z	
Et₃N·3HF	**9**	F	(2)
Et₃N·HX	**10**	Cl	(3)
	11	Br	(4)
	12	I	(5)
HC≡CH	**13**	1/2(C≡C)	(6)
or HC≡CPh	**14**	C≡CPh	(7)

generally take place under mild conditions and with quantitative conversion to the expected products with unoptimized isolated yields ranging from 50 to 90%. The reactions were carried out in THF or toluene depending on the solubility of the reaction product. For the halide-substituted azastannatranes **9–12**, the solubility decreases with decreasing solvent polarity, and in *n*-pentane they are only slightly soluble. As may be expected for the acetylenyl-substituted azastannatranes **13** and **14**, their solubilities in nonpolar solvents are substantial. Except for the
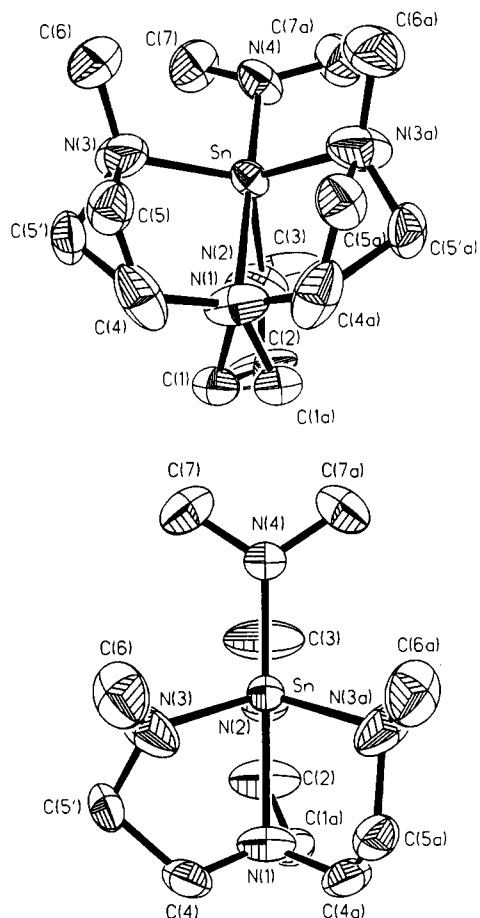
Figure 1. ORTEP drawings of $Me_2NSn(MeNCH_2CH_2)_3N$ (1) showing the disorder of the carbons adjacent to the axial nitrogen (top) and the twist of the NCH_2CH_2N bridges around the C_3 axis upon selection of one of the disordered carbons on each bridge (bottom).

yellowish **12**, the other azastannatranes reported herein are colorless solids.

When reactions 2–7 are carried out in 1:1 stoichiometry, exclusive substitution of the apical dimethylamino group of **1** is observed. Moreover, in no case did excess protic reagent give any detectable reaction at the equatorial amino groups of the azastannatrane cage. These observations clearly show that there are significant differences in the reactivity of the equatorial and the more labile apical amino functionality in these compounds.

It is also interesting in this regard that the reaction of **1** with titanium tetrafluoride or the trifluoroborane–ether adduct (reaction 8) both gave the 1-fluoro-azastannatrane **9** with no NMR-

$$Me_2NSn(NMeCH_2CH_2)_3N \xrightarrow[\text{Et}_2\text{O-BF}_3]{\text{TiF}_4 \text{ or}} 9 \qquad (8)$$
$$\mathbf{1}$$
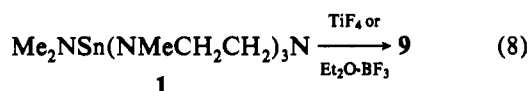
detectable side products. In fact, the exclusive formation of **9** is independent of the stoichiometric ratio of the starting materials.

Attempts to utilize an analogous methatetical reaction for the preparation of a 1-hydroazastannatrane failed. Even at reaction temperatures of –40 °C and less than stoichiometric amounts of $BH_3\cdot NEt_3$, only reduction to elemental tin was observed. This is probably due to the fact that the tin atom in azastannatranes is already rather electron rich, which also accounts for the substantial stability of **9** formed in reaction 8. Thus an electronegative fluorine in the apical position can stabilize the nonbonding orbital of the 3-center 4-electron MO pattern in the F–Sn–N moiety along the 3-fold axis.

Crystal and Molecular Structure of 1. The ORTEP drawing in Figure 1a (top) represents a structure for **1** which is disordered about the crystallographic mirror plane. One NCH_2CH_2N arm

is on the mirror except for C(1), C(1a). The other two arms have C(5), C(5′) and C(5a), C(5′a) disordered over two different sites. By selecting the disordered atoms shown in Figure 1b (bottom), the arms exhibit a twist around the C_3 axis similar to that displayed by the analogue **6**.[1] In the latter structure, however, the "flap" of the envelope conformation formed by each five-membered ring is the carbon adjacent to the equatorial rather than the axial nitrogen. As in **6**, the N(1)–Sn–N(4) angle in **1** (179.8(3)°) is essentially linear. The N_{ax}–Sn bond length in **1** (2.368(3) Å) is within experimental error of that observed for one of the independent molecules of **6** found in the unit cell (2.380(2) Å) but is smaller than that for the second molecule of **6** (2.453(2) Å). Interestingly, this distance in **1** is not lengthened over the shorter analogous distance found in **6**, despite the presumably greater steric hindrance provided by the CH_3N groups in **1** compared with the HN groups in **6**. It is curious that the Me_2N–Sn distance in **1** (2.031(3) Å) is within experimental error (3 esd's) of the average of the Sn–N_{eq} distances (2.038(4) Å), whereas the transannular Sn–N_{ax} bond length is considerably longer (2.368(3) Å). Since the average N_{ax}–Sn–N_{eq} angle (79.4(1)°) and the average Sn–N_{eq} distance (2.058(2) Å) in **1** are within experimental error of those found for **6** (77.8(8)° and 2.038(4) Å, respectively), it would appear that any repulsions between the exocyclic substituents on N_{eq} and the Z group in the two compounds are about the same. Thus the transannular Sn–N_{ax} bond in **1** apparently does not perceptibly lengthen the Sn–N bond trans to it, presumably because the Sn–N_{ax} bond is too long, exceeding its trans counterpart by >0.30 Å, perhaps because of strain in the five-membered rings. In accord with near equality among the four covalent Sn–N bonds in **1** is the observation that the geometries around the equatorial nitrogens (average sum of angles = 359.3(3)°) and the Me_2N nitrogen (sum of angles = 353.6(3)°) are virtually planar, suggesting nearly equal π-bonding possibilities for the two types of nitrogens. On the other hand (see later), the ^{119}Sn chemical shift is strongly influenced by the presence of the transannular interaction.

Mass Spectra. Using EI ionization, all of the new azastannatranes except **12** and **13** display a molecular ion peak, and their identities were confirmed by high-resolution mass spectroscopy. For the iodoazastannatrane **12**, only under CI conditions (NH_3) was the molecular ion peak found. In the case of the symmetrically substituted acetylene **13**, both techniques allowed only fragmentation products to be observed. As was found for the alkyl- and aryl-substituted azastannatranes 2–7,[1] the loss of the apical substituent is a dominant feature of the fragmentation patterns of **9–14**. But in contrast to the alkyl and aryl substituted azastannatranes, the compounds examined herein show rather small relative intensities for all the peaks observed for m/e >99, and generally m/e 99 is the base peak. The latter feature in conjunction with an extensive isotopic peak manifold for ^{116}Sn through ^{124}Sn rendered an interpretation of the high-resolution measurement a rather formidable task, since peaks not superimposed with any other isotopomer (e.g. ^{13}C) or a protonated or deprotonated species (e.g. ±H) are difficult to locate with certainty.

Infrared Spectra. We were hoping that the availability of substituted azastannatranes all possessing approximate C_{3v} molecular symmetry would enable us to gain a more detailed knowledge of the vibrations characteristic of the atrane cage. Having such a series of compounds exhibiting only minor structural differences and all belonging to the same symmetry point group is important, since it is known from the analogous silatranes that the normal modes for their tricyclic atrane frameworks are extremely mixed.[9,10]

As expected, the infrared spectra of azastannatranes **9–14** all display essentially the same absorption bands. (See Experimental

(9) Imbenotte, M.; Palavit, G.; Legrand, P.; Huvenne, J. P.; Fleury, G. *J. Mol. Spectrosc.* **1983**, *102*, 40.

(10) Hencsei, P.; Sebestyen, A. *Main Group Met. Chem.* **1988**, *11*, 243.

Section.) For each of the compounds we also found additional absorption bands related to the vibronic motion of the apical substituent with respect to the central tin atom. In the case of **14**, additional vibrational modes were found for the phenyl group (C=C stretches 1597, 1570, and 1485 cm^{-1}; C—H deformations 761 and 692 cm^{-1}) as well as for the acetylene (ν(C≡C) = 2131 cm^{-1}). For the bis(azastannatranyl)acetylene **13**, no C≡C stretching mode was observed, indicating the expected presence of a center of inversion for this molecule.

The Sn–Z stretching modes of the 1-haloazastannatranes **9–12** were assigned to absorption bands at 515 (Z = F), 304 (Z = Cl), 225 (Z = Br), and 206 cm^{-1} (Z = I), respectively. The bands are shifted to somewhat lower frequencies compared with those of the corresponding halogen-substituted trimethyltin derivatives.[11] The same behvaior was found for 1-halosilatranes compared with their acyclic analogues.[12]

As was noted above, the normal modes are expected to be extremely mixed. Therefore we will give only a tentative assignment of the dominant stretching motion for a few of the observed bands. The Sn–N$_{ax}$ bond stretching coordinate is of special interest, since the corresponding vibration frequency could give some idea of the transannular bond strength. Despite the complex structure of the normal modes for such tricyclic atrane frameworks for silatranes, one absorption band at 348 cm^{-1} was found to have a dominant Si–N$_{ax}$ bond stretching contribution.[9,10] Simply transferring this result to our azastannatrane moiety and assuming a similar force field, an absorption band at approximately 300 cm^{-1} would be predicted. For the 1-haloazastannatranes **9–12**, bands are observed at 302, 304, 305, and 306 cm^{-1}, respectively, which may be viewed as having a potential energy contribution from the Sn–N$_{ax}$ bond stretching coordinate. These absorption bands show only minor shifts on changing the apical group (cf. 298 cm^{-1} for **13** and **14**). The corresponding absorptions reported earlier for **1, 3, 5, 7**, and **8** (297, 303, 296, 299, and 307 cm^{-1}, respectively)[1] fall in the same range.

In principal, the coupling of the Sn–Z stretching coordinate with the cage vibrations should be rather small whereas, for the vibrational coordinates within the cage, a pronounced mixing is expected. This may be visualized by the simple picture of the vibrational motion along the transannular Sn–N$_{ax}$ bond stretching coordinate, which inherently involves a deformation of the three ethylenediamine bridges. Therefore only moderate shifts for absorption bands due to cage vibrations are expected upon changing the apical group. Assuming approximate C_{3v} molecular symmetry, the observed bands fall into a_1 and e symmetry vibrations. As a consequence, the Sn–Z stretching mode can only have symmetry-allowed mixing with the a_1 symmetry vibrations of the cage framework, thereby permitting identification of the latter in some cases. On the basis of this argument, we can assign the pair of absorptions at about 400 and 480 cm^{-1} as a_1 symmetry vibrations (**9**, 406, ---; **10**, 404, 484; **11**, 397, 480; **12**, 394, 475 cm^{-1}). The 480 cm^{-1} absorption band of **9** is probably obscured by the intense Sn–F bond stretching vibration at 515 cm^{-1}. Again, using the above argument, the bands at 508 and 569 cm^{-1} may be assigned as e symmetry vibrations, since they are rather insensitive to changing the apical halogen. The vibrations at 480, 508, and 569 cm^{-1} in these compounds probably possess a significant contribution from the Sn–N$_{eq}$ bond stretching coordinates. For the two acetylene derivatives **13** and **14**, additional absorption bands were found in the region between 500 and 600 cm^{-1}, which are indicative of Sn–C bond stretching vibrations.

NMR Spectra. The ^{1}H, ^{13}C, and ^{119}Sn NMR data for the new azastannatranes **9-14** are summarized in Tables III–V, respec-

Table III. ^{1}H NMR Data for Azastannatranes RSn(CH$_3$NCH$_2^1$CH$_2^2$)$_3$N^a

compd	δ(H^1)	δ(H^2)	$^3J_{H^1H^2}$	δ(CH$_3$)
9	2.59 (84.0)^b	1.99 (2.9)	5.6	3.04 (60.3)
10	2.63 (92.0)	2.02	5.5	3.03 (72.5)
11	2.64 (91.8)	2.06	5.4	2.93 (75.9)
12	2.67 (93.3)	2.06	5.5	2.90 (82.0)
13	2.71 (68.9)	2.22	5.5	3.12 (62.0)
14^c	2.73 (69.1)	2.18	5.5	3.17 (61.3)

^{a} At 293 K in benzene-d_6. δ and J are given in ppm and Hz, respectively. ^{119}Sn–^{1}H coupling constants are given in parentheses. ^{b} $^4J_{FH}$ = 2.8 Hz. ^{c} 6.94–6.96 (pseudotriplet, 3 H, meta and para); 7.51–7.54 (multiplet, 2 H, ortho).

tively. In the ^{1}H NMR spectra, the AA'XX' spin system for the methylene protons of the azastannatrane cage appears as a set of two virtual triplets (virtual point group C_{3v} at room temperature). This pattern is a general feature of the atrane framework.[1,2,13–15] The observed coupling constant of 5.5 Hz for these triplets is independent of the apical group, as was found for a variety of azastannatranes reported earlier.[1] For the series of 1-haloazastannatranes **9–12**, the chemical shifts of the methylene protons decrease with increasing electronegativity of the apical halogen. The opposite trend is found for the protons of the methyl groups adjacent to the equatorial nitrogens. Moreover, as the chemical shifts of these methyl protons increase, their three-bond ^{119}Sn–^{1}H coupling constant decreases. The methylene proton resonances of the acetylene-substituted azastannatranes **13** and **14** are shifted to low field compared with those of the 1-haloazastannatranes **9–12**, but are within the range found for azastannatranes **1–7**.[1] On the other hand, there is a significant difference between the methyl proton shifts of **1, 3, 5** and **7** reported previously[1] and those of the acetylene-substituted derivatives **13** and **14**. For the latter compounds, these resonances are found downfield, compared with those of the 1-haloazastannatranes, whereas for the alkyl and aryl substituted azastannatranes **1, 3, 5**, and **7**, upfield shifts are observed.

The ^{13}C resonances for azastannatranes **9–14** were assigned by J-modulated spin-echo experiments (APT)[16] and by selective proton-decoupling. In the solution ^{13}C NMR spectra, the resonances show only minor shifts upon changing the apical group attached to the tin atom. Both the two- and three-bond ^{119}Sn–^{13}C coupling constants decrease on going from the fluorine to the iodine derivative. Generally, the three-bond ^{119}Sn–^{13}C coupling constant is larger than its two-bond coupling counterpart.

The chemical shifts for the acetylene carbons in **13** and **14** are both at the low-field side of the range observed for a series of acyclic tin functionalities (SnC≡CSn, 115 ppm; SnC≡CR, α-C 75–85 and β-C 97–110 ppm).[17] The $^1J_{SnC}$ coupling constants in **13** and **14** (703.3 and 785.5 Hz) compare quite well with the estimated value of 700 Hz reported in the literature[18] although, in the acyclic series mentioned above, the observed range for $^1J_{SnC}$ is from 388 up to 1168 Hz. The $^2J_{SnC}$ coupling constants for **13** and **14** of 67.2 and 135.9 Hz, respectively, are within the expected range (45–241 Hz).[17]

The ^{13}C chemical shifts of the azastannatranes reported here show only minor changes from solution to the solid state (cf. Table IV). For the methylene carbons, the resonances in the solid state ^{13}C spectra of **11–14** are rather broad. Only in the case of **9** and **10** are two resolved peaks observed. As expected, the anisotropy of these resonances is small, so that no spinning sidebands were observed. The situation is quite different for the

(11) Weidlein, J.; Müller, U.; Dehnicke, K. *Vibration Frequencies*; G. Thieme-Verlag: Stuttgart, Germany, 1981.
(12) Voronkov, M. G.; Baryshok, V. P.; Petukhov, L. P.; Rakhlin, V. I.; Mirskov, R. G.; Pestunovich, V. A. *J. Organomet. Chem.* **1988**, *358*, 39.
(13) Sidorkin, V. F.; Pestunovich, V. A.; Voronkov, M. G. *Magn. Reson. Chem.* **1985**, *23*, 491.
(14) Gudat, D.; Verkade, J. G. *Organometallics* **1989**, *8*, 2772.
(15) Plass, W.; Verkade, J. G. Manuscript in preparation.
(16) Sanders, J. K. M.; Hunter, B. K. *Modern NMR Spectroscopy*; Oxford University Press: Oxford, New York, Frankfurt, 1990.
(17) Wrackmeyer, B. *J. Organomet. Chem.* **1978**, *145*, 183.
(18) Mitchell, T. N.; Walter, G. *J. Organomet. Chem.* **1976**, *121*, 177.

Table IV. ¹³C NMR Data for Azastannatranes RSn(MeNC^{1}H$_2$C^{2}H$_2$)$_3$N[a]

	C^1			C^2			Me		
cmpd	δ_{iso}(solid)	δ(soln)	$\Delta\delta$[b]	δ_{iso}(solid)	δ(soln)	$\Delta\delta$[b]	δ_{iso}(solid)	δ(soln)	$\Delta\delta$[b]
9	49.3	49.7 (16.4)[c]	-0.4	54.4	51.1 (26.8)[c]	3.3	40.2	39.5	0.7
10	49.5	49.9 (9.1)	-0.4	55.1	51.2 (23.1)	3.9	40.1	39.5	0.6
11	51.5[d]	49.7 (4.3)		51.5[d]	51.1 (21.0)		39.2	39.5	-0.3
12	51.0[d]	49.9[e]		51.0[d]	51.6 (18.8)		41.3	40.6	0.7
13[f]	51.3[d]	49.1 (19.4)		51.3[d]	50.8 (23.9)		39.5	39.8 (16.4)	-0.3
14[f]	51.5[d]	49.0 (19.3)		51.5[d]	50.7 (24.2)		39.4	39.9 (14.5)	-0.5

[a] At 293 K. Solution data were obtained in benzene-d_6. δ and J are given in ppm and Hz, respectively. ¹¹⁹Sn–¹³C coupling constants are given in parentheses. [b] $\Delta\delta = \delta$(solid) – δ(soln). [c] $^3J_{FC}$ = 1.0 Hz. [d] Signal is 800 Hz broad. [e] $\Delta\nu_{1/2}$ = 3 Hz. [f] Solution: δ(C≡C) = 120.2 ppm, $^1J_{SnC}$ = 703.3 Hz, $^2J_{SnC}$ = 67.2 Hz. Solid state: δ(C≡C) = 121.6 ppm. [g] Solution: δ(SnC≡C–) = 96.1 ppm, $^1J_{SnC}$ = 785.5 Hz, δ(SnC≡C–) = 112.4 ppm, $^2J_{SnC}$ = 135.9 Hz, δ(ipso C) = 124.5 ppm, $^3J_{SnC}$ = 15.0 Hz, δ(para C) = 128.1 ppm; δ(meta C) = 128.4 ppm, δ(ortho C) = 132.4 ppm, $^4J_{SnC}$ = 7.0 Hz. Solid state: δ(SnC≡C–) = 97.6 ppm, $^1J_{SnC}$ = 800 Hz, δ(SnC≡C–) = 113.5 ppm, δ(ipsoC) = 124.3 ppm, δ(ortho, para, meta C) = 129.7 ppm (750 Hz broad).

Table V. Solid-State and Solution ¹¹⁹Sn NMR Isotropic Chemical Shifts (ppm) for Azastannatranes RSn(MeNCH$_2$CH$_2$)$_3$N[a]

cmpd	δ_{iso}(solid)	$\Delta\delta_{1/2}$(solid)[b]	δ(soln)	$\Delta\delta$[c]
9[d]	-274	500	-261.6	-12.4
10	-192	1400[e]	-180.2	-11.8
11	-200	900	-189.2	-10.8
12	-255	350	-200.7	-54.3
13	-184	450	-182.9	-1.1
14	-172	450	-173.9	1.9

[a] At 293 K. Solution data taken in benzene-d_6 solution. [b] In Hz. [c] $\Delta\delta$ = δ(solid) – δ(soln). [d] ¹¹⁹Sn–¹⁹F coupling constants of 3000 and 2920 Hz were observed in the solid state and solution, respectively. [e] Given for the total width of the 1:1:2 multiplet.

Table VI. ¹³C Shield Tensor Data (ppm) for the Alkyne and Ipso Carbons of PhC$^\beta$≡C$^\alpha$Sn(MeNCH$_2$CH$_2$)$_3$N (14)[a]

	σ_{11}	σ_{22}	σ_{33}	δ_A[b]	η[c]	σ_{iso}
α-C	-240	-185	83	197	0.28	-114
β-C	-201	-122	30	128	0.62	-98
ipso C	-220	-143	-10	114	0.68	-124

[a] The principal axes are chosen according to Haeberlen's notation,[24] where $|\sigma_{33} - \sigma_{iso}| \geq \sigma_1 31 - \sigma_{iso}| \geq |\sigma_{22} - \sigma_{iso}|$. [b] Anisotropy parameter δ_A = $\sigma_{33} - \sigma_{iso}$. [c] Asymmetry parameter η = $(\sigma_{22} - \sigma_{11})\delta_A$.

acetylene and the phenyl carbons of the apical groups in 13 and 14, which all show spinning sideband patterns spanning a range of up to 400 ppm. Unfortunately, a meaningful analysis of these patterns (cf. next section) was only possible for three resonances of the phenylacetylene derivative 14, namely, for the two alkyne carbons and the ipso carbon of the phenyl group (cf. Table VI). The chemical shift tensor of the α alkyne carbon shows a rather high axial symmetry (η = 0.28), in agreement with the 3-fold axis of the atrane framework. Thus it is not surprising that the β alkyne and the ipso carbon both show asymmetry parameters η of 0.62 and 0.68, respectively.

The ¹¹⁹Sn chemical shifts of all the new azastannatranes 9–14 are located in the high-field region, indicating five-coordinate structures and thus confirming the presence of a transannular Sn–N interaction. Generally, the ¹¹⁹Sn chemical shifts of the new azastannatranes reported here and of those reported earlier[1] show remarkable differences upon changing the apical substituent. This situation is quite different from that observed for carbastannatranes RSn(CH$_2$CH$_2$CH$_2$)$_3$N[19] and stannatranes RSn(OCH$_2$CH$_2$)$_3$N.[20] The positions of the ¹¹⁹Sn resonances within the observed range are somewhat unexpected, since the alkyl- and aryl-substituted azastannatrane resonances are found on the downfield side (–90.0 to –150.6 ppm), whereas the 1-haloazastannatrane signals appear at higher fields (–200.7 to –261.6 ppm) together with that of the oxo-bridged derivative 8 (–255.2 ppm[1]). Although this is contrary to the deshielding expected to

Table VII. ¹¹⁹Sn Shielding Tensor Data (ppm) for Azastannatranes RSn(MeNCH$_2$CH$_2$)$_3$N[a]

cmpd	σ_{11}[a]	σ_{22}[a]	σ_{33}[a]	β_A[b]	η[c]	σ_{iso}
10	355	355	-134	-326	0.00	192
13	333	285	-66	-250	0.19	184
14	314	271	-69	-241	0.18	172

[a] The principal axes are chosen according to Haeberlen's notation;[24] see Table IV. [b] Anisotropy parameter δ_A = $\sigma_{33} - \sigma_{iso}$. [c] Asymmetry parameter η = $(\sigma_{22} - \sigma_{11})\delta_A$.

be induced by electronegative substituents, the trend observed within the chlorine, bromine, and iodine triad does reflect this expectation (Table V). The ¹¹⁹Sn chemical shift of –261.6 ppm for the 1-fluoroazastannatrane 9 is exceptional, since it is shifted about 60 ppm upfield with respect to the corresponding shifts for the remaining halides 10–12. Also noteworthy in this context is the rather large $^1J_{SnF}$ value of 2917 Hz for 9. This coupling constant is preferentially measured in the ¹⁹F NMR spectrum because of the better signal-to-noise ratio. Moreover, the observed line broadening of the ¹⁹F resonance for 9 is considerably lower than for its ¹¹⁹Sn resonance.

Solid-State ¹¹⁹Sn NMR spectra. The data obtained from solid-state NMR experiments are given in Tables V and VII. High-resolution solid-state ¹¹⁹Sn CP/MAS NMR spectroscopy is an effective tool for detecting subtle details of structural and electronic properties of tin compounds.[21,22] The changes of the chemical shifts for the new azastannatranes 9–14 on going from the solution to the solid state are with one exception rather modest (<13 ppm), indicating that there is no change in the principal coordination environment of the tin center.[23] Although similar changes were observed for alkyl- and aryl-substituted azastannatranes,[1] the chemical shift changes for the new derivatives herein are opposite in direction, namely, to lower field in solution (cf. Table V). The 1-iodo-azastannatrane 12, with an upfield shift of about 54 ppm to the solid state from solution is still within the five-coordinate range and may be attributed to packing effects. Thus elongation of the transannular Sn–N$_{ax}$ bond in PhSn-(MeNCH$_2$CH$_2$)$_3$N by 7 pm in one of the two molecules of the unit cell was found to move the isotropic chemical shift about 20 ppm downfield.[1]

The anisotropic nature of the chemical shielding is responsible for the pattern normally observed in spectra of stationary powder samples.[24] Singularities found in such a powder pattern correspond to the diagonal elements of the chemical shielding tensor in the principal axis system (PAS). Spinning at the magic-angle with a speed below the powder line width causes the pattern to break up into an isotropic line σ_{iso}, flanked by spinning sidebands.

(19) Mügge, C.; Pepermans, H.; Gielen, M.; Willem, R.; Tzschach, A.; Jurkschat, K. *Z. Anorg. Allg. Chem.* **1988**, *567*, 122.
(20) Jurkschat, K.; Mügge, C.; Tzschach, A.; Zschunke, A.; Fischer, G. W. *Z. Anorg. Allg. Chem.* **1980**, *463*, 123.
(21) Apperley, D. C.; Davies, N. A.; Harris, R. K.; Birmah, A. K.; Eller, S.; Fischer, R. D. *Organometallics* **1990**, *9*, 2672.
(22) Davies, J. A.; Dutremez, S. *Coord. Chem. Rev.* **1992**, *114*, 201.
(23) Harris, R. K.; Sebald, A.; Furlani, D.; Tagliavini, G. *Organometallics* **1988**, *7*, 388.
(24) Haeberlen, U. *High Resolution NMR in Solids*; Advances inMagnetic Resonance Supplement; Academic Press: New York, 1976.

The intensities of these spinning sidebands are related to the chemical shielding tensor, thereby providing the opportunity to extract its parameters by graphical analysis.[25] The principal chemical shielding tensor elements σ_{11}, σ_{22}, and σ_{33} are denoted by the convention:

$$|\sigma_{33} - \sigma_{iso}| \geq |\sigma_{11} - \sigma_{iso}| \geq |\sigma_{22} - \sigma_{iso}| \qquad (9)$$

The shielding tensor may be written as a set of parameters reflecting its symmetry and thus be more suitable for chemical purposes, such as for the comparison of local chemical environments. The three parameters, the isotropic chemical shielding (σ_{iso}), the anisotropy parameter (δ_A), and the asymmetry parameter (η), are given by the relations:

$$\sigma_{iso} = {}^1/_3(\sigma_{11} + \sigma_{22} + \sigma_{33}) \qquad (10)$$

$$\delta_A = \sigma_{33} - \sigma_{iso} \qquad (11)$$

$$\eta = (\sigma_{22} - \sigma_{11})/\delta_A \qquad (12)$$

The observed signal-to-noise ratio, together with the almost vanishingly small intensity of the centerband in some cases, allowed a meaningful analysis of the spinning sideband patterns only for azastannatranes 10, 13, and 14. The chemical shielding parameters for these compounds are listed in Table VII. For the 1-fluoroazastannatrane 9, a simple evaluation of the chemical shielding tensor parameters is prohibited by the observation that the two sideband manifolds feature different intensity distributions.[26,27] The splitting of the centerband gives a $^1J_{SnF}$ coupling constant of 3000 Hz, which is in good agreement with the solution value. The high-field spinning sideband manifold is spread over a range of 490 ppm, whereas the low-field counterpart displays a width that is 90 ppm smaller. The chemical shielding tensors of the azastannatranes examined herein in general show a greater anisotropy ($|\delta_A| > 240$ ppm) than the azastannatranes 1-7 which have a range from 90 to 220 ppm. Moreover, the observed asymmetry parameters are considerably smaller in 10, 13, and 14 and the 1-chloroazastannatrane 10 displays an axially symmetric spinning sideband pattern. The asymmetry parameter of 0.18 for the ^{119}Sn shielding tensor of 14 (indicating a nearly axial symmetry) is consistent with the low symmetry parameter observed for the ^{13}C shielding tensor of the carbon bonded to it (cf. Table VI).

The effect of quadrupolar nuclei on the spectra of spin $^1/_2$ nuclei is well documented for the ^{13}C–^{14}N pair.[28] The MAS experiment for quadrupolar nuclei does not suppress dipolar interactions with half-integer nuclei, which generally give rise to 1:2 or 2:1 broadened doublets for ^{13}C spectra of nuclei coupled to ^{14}N. Similar residual dipolar coupling effects have also been seen for other pairs of nuclei such as ^{31}P–^{63,65}Cu,[29] ^{31}P–^{55}Mn,[30] ^{13}C–^{51}V,[15] and ^{119}Sn–^{35,37}Cl.[23,31] Such residual dipolar effects could in principle also be expected for our 1-haloazastannatranes 10–12. However, only the solid state spectrum of the 1-chloroazastannatrane 10 shows a resolved splitting of the centerband into a broadened 1:1:2 asymmetric three-line pattern. Splitting due to interaction of a spin $^1/_2$ nucleus with a quadrupolar nucleus generally can only be observed when the relaxation of the quadrupolar nucleus is sufficiently slow, since very fast relaxation leads to "self-decoupling"[23] in the limiting case. Since neither

the bromo derivative 11 nor the iodo derivative 12 shows any splitting, such self-decoupling may be occurring. On the other hand, the centerbands in both spectra show considerable line broadening (cf. Table V), possibly indicating unresolved residual coupling effects.

For pairs of spin $^1/_2$ and quadrupolar nuclei, two possible types of interaction must be considered, namely, the scalar or indirect coupling (J coupling) and the dipolar or direct coupling, since both types may be present. Distortions of a multiplet caused by such interactions will not be completely averaged by MAS when the spin states of the quadrupolar nucleus are no longer quantized along the external magnetic field (i.e., z axis). This situation arises when the Zeeman and the quadrupole interactions for the quadrupolar nucleus are of the same order of magnitude. Accordingly, anisotropy in the scalar coupling also will not be removed entirely by MAS in such circumstances. For the analysis of MAS NMR spectra of spin $^1/_2$ nuclei scalar-coupled to quadrupolar nuclei under conditions where second-order effects are important, a pertubation theory approach can be utilized.[32,33] Using this first-order pertubation treatment to evaluate the CP/MAS NMR spectrum of 10 leads to approximate values for the isotropic scalar coupling constant ($J_{iso} = 260$ Hz) and the parameter characterizing the distortion of the multiplet ($d = 130$ Hz). The value of J_{iso} found for 10 is in good agreement with a value of 220 Hz estimated for a series of ClSnR$_3$ compounds (R = alkyl and aryl).[23] Assuming axial symmetry for the quadrupole tensor of chlorine, together with a collinear arrangement of the z axis of both the quadrupolar and the scalar coupling tensors along the Sn–Cl bond vector, the distortion parameter d is given by[32] eq 13, wherein Z_V is the Zeeman frequency of ^{35}Cl

$$d = \frac{-\chi}{10 Z_V}(-\Delta J + 3D) \qquad (13)$$

in the applied field, ΔJ is the anisotropy of the scalar coupling, $D = (\mu_0/4\pi)(\gamma_{Sn}\gamma_{Cl}/r_{Sn-Cl}{}^3)(h/4\pi^2)$ is the dipolar coupling constant, and χ is the quadrupolar coupling constant of ^{35}Cl. Even assuming that the scalar coupling is completely isotropic leaves two unknown variables in the above equation, namely, the quadrupolar coupling constant χ and the dipolar coupling constant D. A rough estimate of $D = -250$ Hz can be calculated by assuming an Sn–Cl bond length of 261.3 pm as found in a chlorocarbastannatrane.[34] This would lead to a quadrupolar coupling constant $\chi = -51.0$ MHz, which is rather large compared to the -30 to -40 MHz range normally found in chlorotin compounds.[35] Consequently, the effect of ΔJ should also be taken into account. In that case, the above equation shows that ΔJ should be 290 Hz. Since the estimate of 260 pm can be considered as an upper limit for the Sn–Cl bond length in pentacoordinated tin compounds,[34,36–38] we can use 235 pm[33] for the lower limit because 239 pm is the sum of the covalent radii.[39] Using 235 pm for the Sn–Cl bond length, D would be estimated to be -340 Hz and the quadrupolar coupling constant χ would be estimated to be -37.5 MHz. Using this χ value, no ΔJ effect appears to be operative. Thus the values given here for the dipolar coupling constant D and the quadrupolar coupling constant χ can only serve as limiting estimates.

Mobility of the Azastannatrane Framework. In addition to the transannular Sn–N bond, the racemization of the chiral

(25) Herzfeld, J.; Berger, A. E. *J. Chem. Phys.* **1980**, *73*, 6021.
(26) Iwamiya, J. H.; Maciel, G. E. *J. Magn. Reson.* **1991**, *92*, 590.
(27) Harris, R. K.; Packer, K. J.; Reams, P. *Chem. Phys. Lett.* **1985**, *115*, 16.
(28) Hexem, J. G.; Frey, M. H.; Opella, S. J. *J. Chem. Phys.* **1982**, *77*, 3847.
(29) Menger, E. M.; Veeman, W. S. *J. Magn. Reson.* **1982**, *46*, 257.
(30) Lindner, E.; Fawzi, R.; Mayer, H. A.; Eichele, K.; Pohmer, K. *Inorg. Chem.* **1991**, *30*, 1102.
(31) Komoroski, R. A.; Parker, R. G.; Mazany, A. M. *J. Magn. Reson.* **1987**, *73*, 389.

(32) Olivieri, A. C. *J. Magn. Reson.* **1989**, *81*, 201.
(33) Apperley, D. C.; Haiping, B.; Harris, R. K. *Mol. Phys.* **1989**, *68*, 1277.
(34) Jurkschat, K.; Tzschach, A.; Meunier-Piret, J.; van Meerssche, M. *J. Organomet. Chem.* **1985**, *290*, 285.
(35) Green, P. J.; Graybeal, J. D. *J. Am. Chem. Soc.* **1967**, *89*, 4305.
(36) Swisher, R. G.; Holmes, R. R. *Organometallics* **1984**, *3*, 365.
(37) Domazetis, G.; MacKay, M. F.; Magee, R. J.; James, B. D. *Inorg. Chim. Acta* **1979**, *34*, L247.
(38) Hulme, R. *J. Chem. Soc.* **1963**, 1524.
(39) Huheey, J. E. *Inorganic Chemistry, Principles of Structure and Reactivity*; Harper & Row, Publishers, Inc.: New York, 1983.

Table VIII. Free Activation Enethalpies $\Delta G_{T_c}^*$ (kJ/mol) of Racemization for Azastannatranes RSn(MeNCH$_2$CH$_2$)$_3$N^a

cmpd	T_c^b	$\Delta\nu^c$	$\Delta G_{T_c}^*$
9	186	227	35.4
10	188	229	35.6
11	187	227	35.4
13	193	213	36.7
14	193	248	36.4

^{a} Calculated from the coalescence of the ^{1}H resonances of the N(CH$_2$)$_3$ groups in toluene-d_8. In all cases, it was possible to supercool the toluene-d_8 solutions to about 170 K without freezing. ^{b} T_c in K; $\Delta T_c = \pm 1$K. ^{c} $\Delta\nu$ in Hz; $\Delta(\Delta\delta) = \pm 10$ Hz.

molecular skeleton is also a characteristic feature of azastannatrane frameworks. This molecular mobility is manifested in the appearance of the AA'XX' spin system for the methylene protons of the azastannatrane cage as a pseudotriplet at room temperature. Upon cooling, the spectra of azastannatranes 9–14 show broadening for the two methylene pseudotriplets, eventually forming two broad singlets, while all the other resonances remain sharp and well resolved down to 170 K. This behavior is indicative of a racemization process.[1,2,19] The free activation enthalpies ΔG^* of racemization, summarized for the new azastannatranes in Table VIII, are based on the coalescence of the methylene protons adjacent to the axial nitrogen. For the 1-halo-azastannatranes 9–12, the free activation enthalpies are virtually the same in all four cases ($\Delta G_{T_c}^* \approx 35$ kJ/mol) whereas, for the acetylenyl-substituted derivatives 13 and 14, the barrier is about 1 kJ/mol higher. The $\Delta G_{T_c}^*$ values for 9–14 are found at the upper limit compared with the range 33–36 kJ/mol observed for the azastannatranes (1–7) reported previously.[1] Somewhat higher $\Delta G_{T_c}^*$ values are observed for the equatorial N-methyl-substituted azastannatrane frameworks than for the N-hydrogen derivatives. The only two exceptions are the dimethylamino derivative 1 (33.3 kJ/mol) and the phenyl derivative 7 (33.6 kJ/mol). Interestingly, these exceptions correspond to those derivatives showing a significant distortion of the local C_{3v} symmetry at the tin atom.

Although pronounced deviations for the racemization enthalpies of various azastannatranes were found[1] (see also Table VIII), the rigidity of the atrane skeleton depends mainly on the nature of the central atom of the atrane framework. For transition metal azatranes, the barrier is about 5–6 kJ/mol higher[2,15] than for azastannatranes and carbastannatranes.[19] It is particularly noteworthy that racemization does not depend on the strength of the transannular interaction between the axial nitrogen and the central cage atom. This is strongly indicated by the invariant $\Delta G_{T_c}^*$ values observed for the halogen derivatives 9–12.

Conclusions. It has been shown that azastannatrane 1 undergoes a facile nucleophilic substitution reaction on the apical position, yielding a variety of new derivatives. It was possible to undertake a detailed study of the spectroscopic properties of the azastannatrane framework, owing to the availability of a systematic series of apically substituted derivatives. The absorption band found at 300 cm^{-1} is assigned to a vibration mode having a significant contribution from the axial Sn–N$_{ax}$ bond stretching coordinate. The cage vibrations, however, are extremely mixed. A strong transannular tin–nitrogen bond is indicated by solution and solid state ^{119}Sn NMR studies. The racemization barrier for the azatrane framework in these compounds is found to be considerably lower than those for their transition metal analogues.